Path optimization for the Laser Powder Bed Fusion (LPBF) additive manufacturing process

PhD funded by SOFIA project

Mathilde Boissier[1,2], Grégoire Allaire[1], Christophe Tournier[2]

[1]CMAP, Ecole Polytechnique, France
[2]LURPA, ENS Paris Saclay, France

12/09/2019

Introduction

The LPBF process

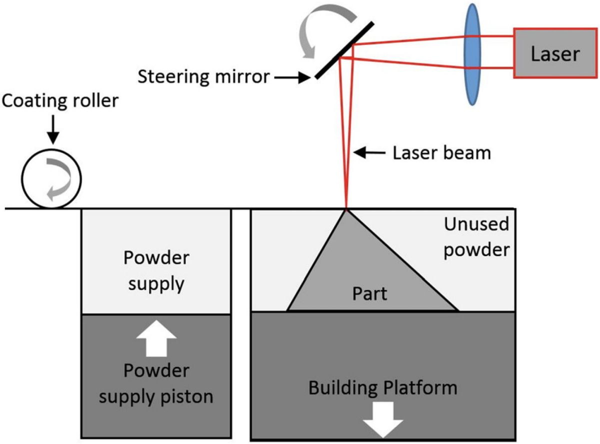

Process description (Bikas, Stavropoulos, and Chryssolouris 2016)

Laser path

State of the art : (Ding et al. 2015; Liu et al. 2018)

parallel contour spiral continuous Medial Axis Transformation

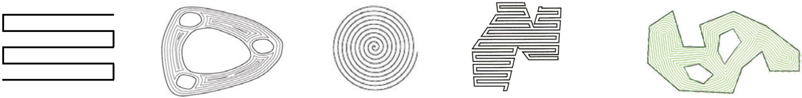

- Allocation of these paths to domain cells,
- Velocity and power optimization,
- "Live" path adaptation.

Goal : path optimization without basing it upon any pattern.

Outline

Model

LPBF modelization

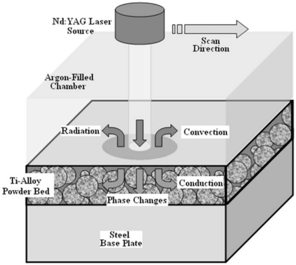

LPBF process
(Roberts et al. 2009)

Microscopic scale
(Megahed et al. 2016; DebRoy et al. 2018)

- accurate model for the change of state, melting pool,
- 4 states considered: powder, solid, liquid, gaz.

Macrocospic scale
(Van Belle 2013; Megahed et al. 2016; Allaire and Jakabčin 2018)

- conduction, convection and radiation
- 2 states considered: powder and solid.

Stakes at a macroscopic scale:

- **thermomechanics**: thermal expansion, residual stresses, solidification of the layer,
- **kinematics**: minimal execution time, easy to create.

SOFIA CMAP LURPA

Macroscopic 2D model (in the layer plane)

Heat equation (conduction only):

$$\begin{cases} \rho_{pow}.c_{p,pow}.\partial_t T - \nabla \cdot (\lambda_{pow}.\nabla T) + \frac{\lambda_{sol}}{L\Delta Z} T = \frac{Q}{L}, & (t,x) \in (0,t_F) \times \Sigma, \\ \lambda_{pow}.\nabla T \cdot n = 0, & (t,x) \in (0,t_F) \times \partial\Sigma, \\ T(0,x) = T_{init}(x) & x \in \Sigma. \end{cases}$$

Source model: $Q(t,x) = P \exp\left(-\delta|x-u(t)|^2\right)$, ($u(t)$ the laser path).

Physical characteristics time independent (powder or solid value chosen depending on the context).

Constraints to satisfy:

- change of state: $\forall x \in D, \exists t \quad \text{such that} \quad T(t,x) > T_\Phi$,
- thermal expansion: $\forall x \in D, \forall t, \quad T(t,x) < T_M$,
- ~~residual stresses.~~

Steady problem

Optimization problem to consider

Steady model: source on the whole trajectory at the same time (heating thread).

Objective : vary the path Γ in order to minimize its length ($J(\Gamma)$) while satisfying the change of phase (C_Φ) and maximal temperature constraints (C_M).

$$\min_{\Gamma} J(\Gamma) = \int_\Gamma ds$$

while satisfying the constraints

$$\begin{cases} C_{\Phi,st} = \int_\Sigma \left[(T_\Phi - T)^+\right]^2 dx = 0 & (T > T_\Phi), \\ C_{M,st} = \int_\Sigma \left[(T - T_M)^+\right]^2 dx = 0 & (T < T_M). \end{cases}$$

and T solution of:

$$\begin{cases} -\nabla \cdot (\lambda_{pow.} \nabla T) + \frac{\lambda_{sol.}}{L \Delta Z} T = \frac{P}{L} \chi_\Gamma, & (t, x) \in (0, t_F) \times \Sigma \\ \lambda_{pow.} \nabla T \cdot n = 0 & (t, x) \in (0, t_F) \times \partial\Sigma \end{cases}$$

Computation of the speed of variation: shape optimization (Henrot and Pierre (2018) and Allaire, Jouve, and Toader (2004))

Shape optimization: variation with respect to a vector field ϑ,

Γ regular curve with chosen orientation, which tangent is τ, which normal is n and curvature κ with A and B its endpoints.

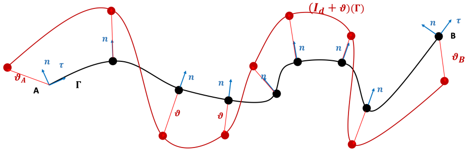

- Shape derivative of $J(\Gamma) = \int_\Gamma f(s)ds$:

$$J'(\Gamma)(\vartheta) = \int_\Gamma [\partial_n f + \kappa f] \, \vartheta \cdot n ds + f(B)\vartheta(B) \cdot \tau(B) - f(A)\vartheta(A) \cdot \tau(A)$$

- Then:

$$J(\Gamma^{n+1}) = J(\Gamma^n) + J'(\Gamma^n)(\vartheta) + o(\vartheta)$$

and ϑ is chosen such that $J(\Gamma^{n+1}) \leq J(\Gamma^n)$.

Results

Values: (Van Belle 2013; Allaire and Jakabčin 2018)
$\lambda_{sol.} = 15 W.m^{-1}K^{-1}$, $\lambda_{pow.} = 0.25 W.m^{-1}K^{-1}$, $L = 10cm$, $\Delta Z = 1m$, $P = 800 W.m^{-2}$, $T_\Phi = 1700K$, $T_M = 2000K$, $T_{init} = 500K$.

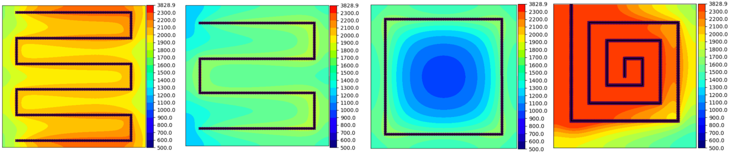

$$N(C_{\Phi,st}) = \sqrt{\frac{C_{\phi,st}}{|\Sigma| T_\Phi^2}}, \qquad N(C_{M,st}) = \sqrt{\frac{C_{M,st}}{|\Sigma| T_M^2}}$$

Case	Length (m)	$N(C_{\phi,st})$	$N(C_{M,st})$
Reference (non optimized)	1.14	$1.97e-5$	$3.29e-2$
Zigzag initialization	1.00	$3.63e-5$	$2.50e-5$
Contour initialization	1.00	$2.20e-4$	$2.92e-4$
Spiral initialization	1.02	$1.67e-9$	$8.66e-7$

Results

Values: (Van Belle 2013; Allaire and Jakabčin 2018)
$\lambda_{sol.} = 15W.m^{-1}K^{-1}$, $\lambda_{pow.} = 0.25W.m^{-1}K^{-1}$, $L = 10cm$, $\Delta Z = 1m$, $P = 800W.m^{-2}$,
$T_\Phi = 1700K$, $T_M = 2000K$, $T_{init} = 500K$.

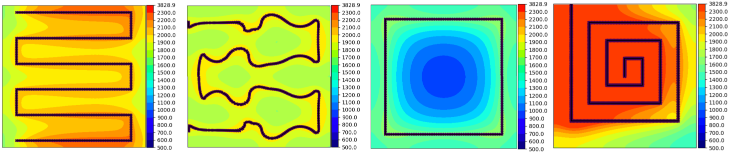

$$N(C_{\Phi,st}) = \sqrt{\frac{C_{\phi,st}}{|\Sigma| T_\Phi^2}}, \qquad N(C_{M,st}) = \sqrt{\frac{C_{M,st}}{|\Sigma| T_M^2}}$$

Case	Length (m)	$N(C_{\phi,st})$	$N(C_{M,st})$
Reference (non optimized)	1.14	$1.97e-5$	$3.29e-2$
Zigzag initialization	1.00	$3.63e-5$	$2.50e-5$
Contour initialization	1.00	$2.20e-4$	$2.92e-4$
Spiral initialization	1.02	$1.67e-9$	$8.66e-7$

Results

Values: (Van Belle 2013; Allaire and Jakabčin 2018)
$\lambda_{sol.} = 15W.m^{-1}K^{-1}$, $\lambda_{pow.} = 0.25W.m^{-1}K^{-1}$, $L = 10cm$, $\Delta Z = 1m$, $P = 800W.m^{-2}$,
$T_\Phi = 1700K$, $T_M = 2000K$, $T_{init} = 500K$.

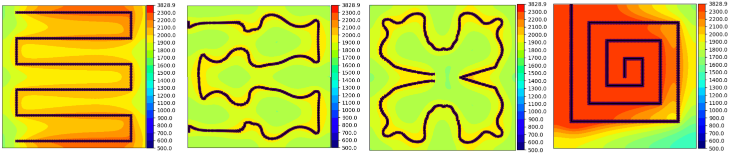

$$N(C_{\Phi,st}) = \sqrt{\frac{C_{\phi,st}}{|\Sigma|T_\Phi^2}}, \qquad N(C_{M,st}) = \sqrt{\frac{C_{M,st}}{|\Sigma|T_M^2}}$$

Case	Length (m)	$N(C_{\phi,st})$	$N(C_{M,st})$
Reference (non optimized)	1.14	$1.97e-5$	$3.29e-2$
Zigzag initialization	1.00	$3.63e-5$	$2.50e-5$
Contour initialization	1.00	$2.20e-4$	$2.92e-4$
Spiral initialization	1.02	$1.67e-9$	$8.66e-7$

Results

Values: (Van Belle 2013; Allaire and Jakabčin 2018)
$\lambda_{sol.} = 15W.m^{-1}K^{-1}$, $\lambda_{pow.} = 0.25W.m^{-1}K^{-1}$, $L = 10cm$, $\Delta Z = 1m$, $P = 800W.m^{-2}$,
$T_\Phi = 1700K$, $T_M = 2000K$, $T_{init} = 500K$.

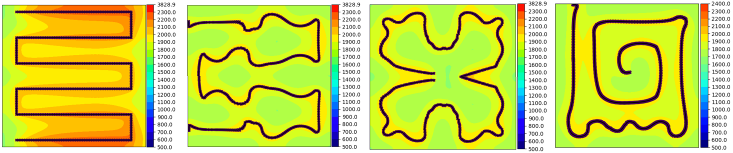

$$N(C_{\Phi,st}) = \sqrt{\frac{C_{\phi,st}}{|\Sigma|T_\Phi^2}}, \qquad N(C_{M,st}) = \sqrt{\frac{C_{M,st}}{|\Sigma|T_M^2}}$$

Case	Length (m)	$N(C_{\phi,st})$	$N(C_{M,st})$
Reference (non optimized)	1.14	$1.97e-5$	$3.29e-2$
Zigzag initialization	1.00	$3.63e-5$	$2.50e-5$
Contour initialization	1.00	$2.20e-4$	$2.92e-4$
Spiral initialization	1.02	$1.67e-9$	$8.66e-7$

Results

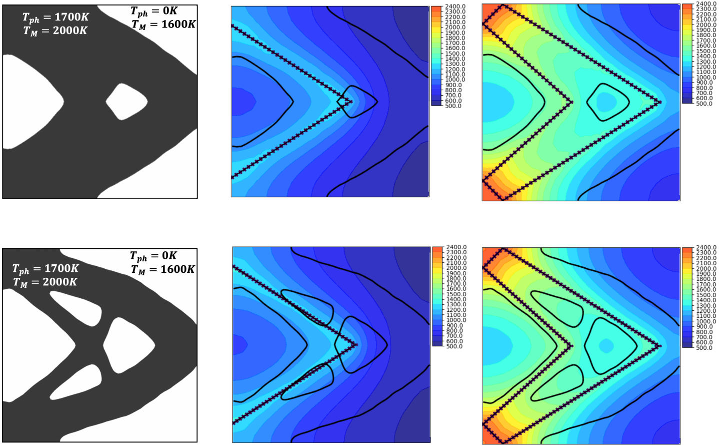
$T_{ph} = 1700K$
$T_M = 2000K$
$T_{ph} = 0K$
$T_M = 1600K$
2400.0 2300.0 2200.0 2100.0 2000.0 1900.0 1800.0 1700.0 1600.0 1500.0 1400.0 1300.0 1200.0 1100.0 1000.0 900.0 800.0 700.0 600.0 500.0
$T_{ph} = 1700K$
$T_M = 2000K$
$T_{ph} = 0K$
$T_M = 1600K$

Results

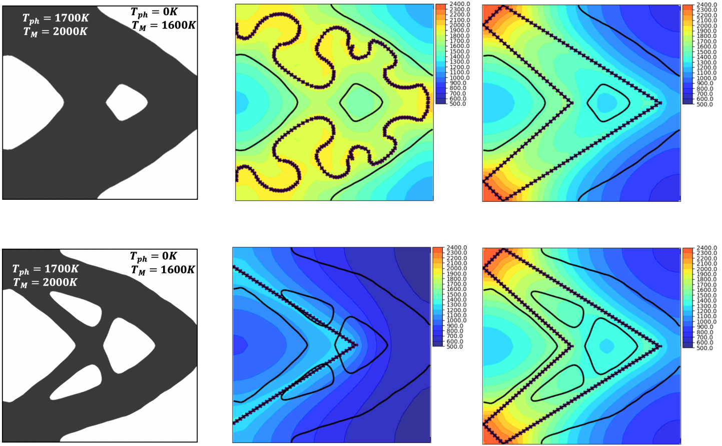
$T_{ph} = 1700K$
$T_M = 2000K$
$T_{ph} = 0K$
$T_M = 1600K$
$T_{ph} = 1700K$
$T_M = 2000K$
$T_{ph} = 0K$
$T_M = 1600K$
2400.0
2300.0
2200.0
2100.0
2000.0
1900.0
1800.0
1700.0
1600.0
1500.0
1400.0
1300.0
1200.0
1100.0
1000.0
900.0
800.0
700.0
600.0
500.0

Results

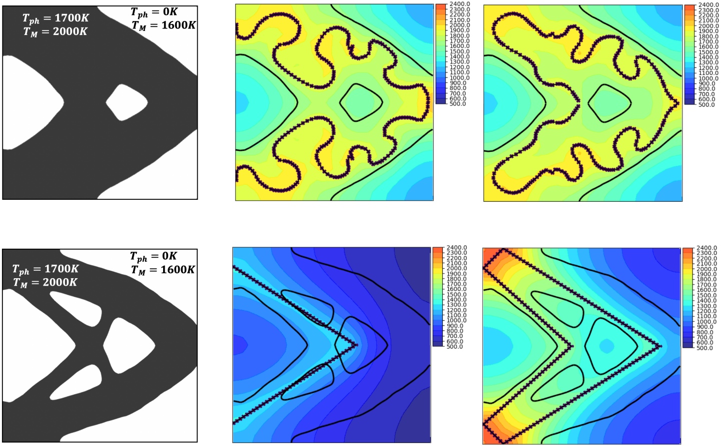
$T_{ph} = 1700K$
$T_M = 2000K$
$T_{ph} = 0K$
$T_M = 1600K$
2400.0 2300.0 2200.0 2100.0 2000.0 1900.0 1800.0 1700.0 1600.0 1500.0 1400.0 1300.0 1200.0 1100.0 1000.0 900.0 800.0 700.0 600.0 500.0
$T_{ph} = 1700K$
$T_M = 2000K$
$T_{ph} = 0K$
$T_M = 1600K$

Results

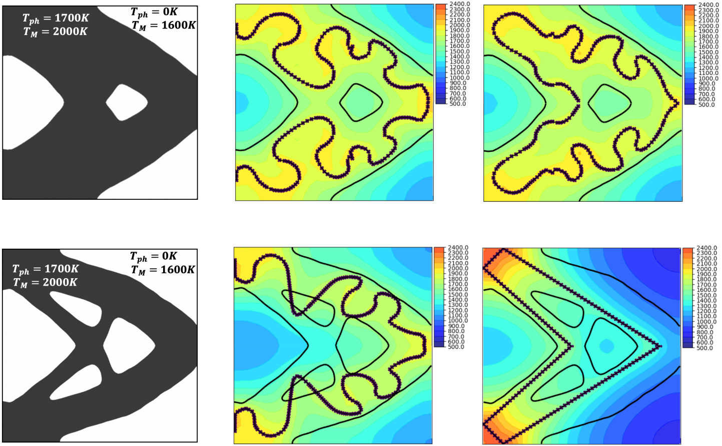
$T_{ph} = 1700K$
$T_M = 2000K$
$T_{ph} = 0K$
$T_M = 1600K$
$T_{ph} = 1700K$
$T_M = 2000K$
$T_{ph} = 0K$
$T_M = 1600K$
2400.0 2300.0 2200.0 2100.0 2000.0 1900.0 1800.0 1700.0 1600.0 1500.0 1400.0 1300.0 1200.0 1100.0 1000.0 900.0 800.0 700.0 600.0 500.0

Results

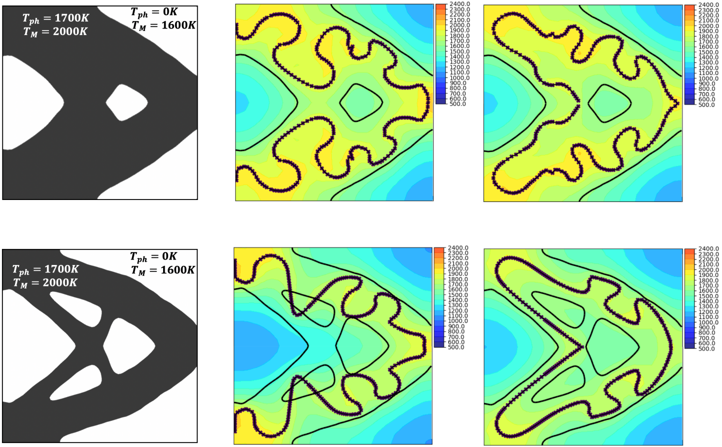
$T_{ph} = 1700K$
$T_M = 2000K$
$T_{ph} = 0K$
$T_M = 1600K$
$T_{ph} = 1700K$
$T_M = 2000K$
$T_{ph} = 0K$
$T_M = 1600K$

Unsteady problem

Unsteady context (laser speed V fixed)

Objectives:

- final time: $L_g = t_F$
- change of state: $\forall x \in D, \exists t \in [0, t_F]$ such that $T(t,x) > T_\Phi$,

$$C_\Phi = \int_\Sigma \left[\left(T_\Phi - \max_t(|T(.,x)|) \right)^+ \right]^2 dx \approx \int_\Sigma \left[\left(T_\Phi - \|T(.,x)\|_{L^p(0,t_F)} \right)^+ \right]^2 dx.$$

- thermal expansion: $\forall (x,t) \in \Sigma \times [0, t_F], \ T(t,x) < T_M$,

$$C_M = \int_\Sigma \int_0^{t_F} \left[(T(t,x) - T_M)^+ \right]^2 dt dx.$$

Equations:

$$\begin{cases} \rho_{pow}.c_{p,pow}.\partial_t T - \nabla \cdot (\lambda_{pow}.\nabla T) + \frac{\lambda_{sol}}{L \Delta Z} T = \frac{Q(t,x)}{L}, & (t,x) \in (0,t_F) \times \Sigma, \\ \lambda_{pow}.\nabla T \cdot n = 0, & (t,x) \in (0,t_F) \times \partial\Sigma \\ T(0,x) = T_{init}(x) & x \in \Sigma. \end{cases}$$

with $Q(t,x) = P \exp\left(-\delta |x - u(t)|^2 \right)$

$$\begin{cases} \dot{u}(t) = V \tau(t) & t \in [t_1, t_F] \\ u(t_1) = \tilde{u}. \end{cases}$$

Optimal control of the line (Wendl, Pesch, and Rund (2010))

Control of the line: angle θ, formed by the horizontal and the tangent at each point.

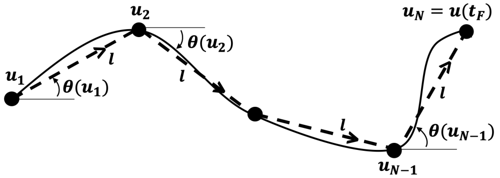

$$\min_{\theta, t_F, \tilde{u}} J = \Lambda_F(t_F) + \Lambda_\Phi(C_\Phi) + \Lambda_M(C_M),$$

while satisfying:

$$\begin{cases} \rho_{pow}.c_{p,pow}.\partial_t T - \nabla\cdot(\lambda_{pow}.\nabla T) + \frac{\lambda_{sol}}{L\Delta Z} T = \frac{Q(t,x)}{L}, & (t,x) \in (0,t_F)\times\Sigma, \\ \lambda_{pow}.\nabla T\cdot n = 0, & (t,x)\in(0,t_F)\times\partial\Sigma, \\ T(0,x) = T_{init}(x) & x\in\Sigma. \end{cases}$$

with $Q(t,x) = P\exp\left(-\delta|x-u(t)|^2\right)$, where the path equation u is given by:

$$\begin{cases} \dot{u}(t) = VF(\theta(t)) = V\left(\cos(\theta(t)), \sin(\theta(t))\right), & \forall t\in(t_1,t_F) \\ u(t_1) = \tilde{u} \end{cases}$$

Results:

Values: (not realistic but efficient to test the algorithm)

$\lambda_{sol.} = 10000 W.m^{-1}K^{-1}, \quad \lambda_{pow.} = 10000 W.m^{-1}K^{-1},$

$\rho_{sol.} = \rho_{pow.} = 8000 kg.m^{-3},$

$c_{sol.} = c_{pow.} = 450 J.kg^{-1}.K^{-1}$

$L = 10cm, \quad \Delta Z = 10cm, \quad P = 76800000 * (10^4) W.m^{-2},$

$T_\Phi = 773K, \quad T_{init} = 303K., \quad T_M = 2773, \quad p = 8.$

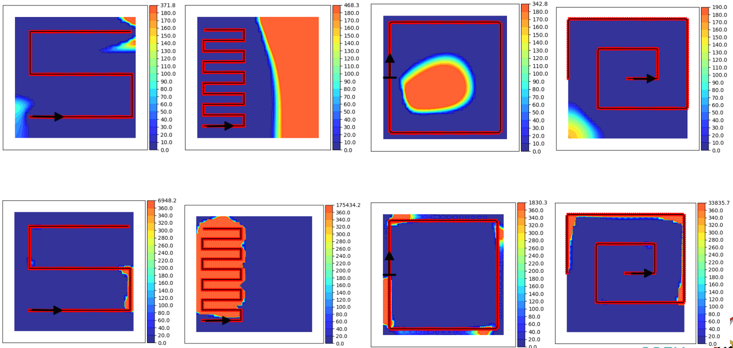

Results:

Values: (not realistic but efficient to test the algorithm)

$\lambda_{sol.} = 10000 W.m^{-1}K^{-1}, \quad \lambda_{pow.} = 10000 W.m^{-1}K^{-1},$

$\rho_{sol.} = \rho_{pow.} = 8000 kg.m^{-3},$

$c_{sol.} = c_{pow.} = 450 J.kg^{-1}.K^{-1}$

$L = 10cm, \quad \Delta Z = 10cm, \quad P = 76800000 * (10^4) W.m^{-2},$

$T_\Phi = 773K, \quad T_{init} = 303K., \quad T_M = 2773, \quad p = 8.$

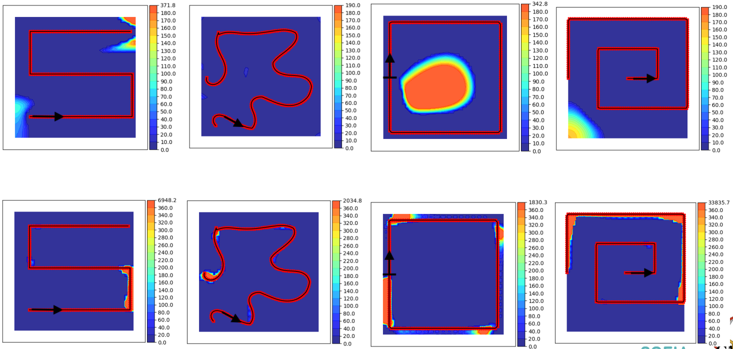

Results:

Values: (not realistic but efficient to test the algorithm)

$\lambda_{sol.} = 10000W.m^{-1}K^{-1}, \quad \lambda_{pow.} = 10000W.m^{-1}K^{-1},$

$\rho_{sol.} = \rho_{pow.} = 8000kg.m^{-3},$

$c_{sol.} = c_{pow.} = 450J.kg^{-1}.K^{-1}$

$L = 10cm, \quad \Delta Z = 10cm, \quad P = 76800000 * (10^4)W.m^{-2},$

$T_\Phi = 773K, \quad T_{init} = 303K., \quad T_M = 2773, \quad p = 8.$

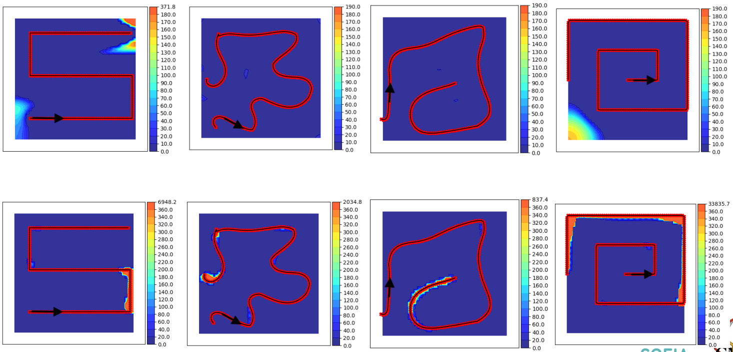

Results:

Values: (not realistic but efficient to test the algorithm)

$\lambda_{sol.} = 10000 W.m^{-1}K^{-1}, \quad \lambda_{pow.} = 10000 W.m^{-1}K^{-1},$

$\rho_{sol.} = \rho_{pow.} = 8000 kg.m^{-3},$

$c_{sol.} = c_{pow.} = 450 J.kg^{-1}.K^{-1}$

$L = 10cm, \quad \Delta Z = 10cm, \quad P = 76800000 * (10^4) W.m^{-2},$

$T_\Phi = 773K, \quad T_{init} = 303K., \quad T_M = 2773, \quad p = 8.$

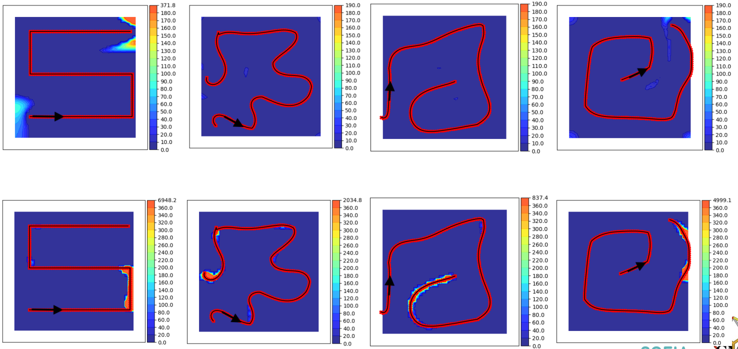

Conclusion and perspectives

Perspectives

Short terms perspectives:

- steady case:
  - adding more realistic constraints (geometrical, thermal et mechanical),
  - allow for the splitting of the path and gathering many,
  - adapt the curve meshing to the industrial requirements,
  - make the 2D case evolve to a layer by layer 3D optimization.
- unsteady case:
  - improve the optimal control model,
  - consider the dependence in time of the physical coefficients,
  - perspectives from the steady case.

Long term perspectives:

- coupling shape optimization to path optimization,
- optimize a line in 3D.

Références I

- Allaire, Grégoire and Lukas Jakabčin (2018). "Taking into Account Thermal Residual Stresses in Topology Optimization of Structures Built by Additive Manufacturing". In: **Mathematical Models and Methods in Applied Sciences** 28.12, pp. 2313–2366.
- Allaire, Grégoire, François Jouve, and Anca-Maria Toader (2004). "Structural Optimization Using Sensitivity Analysis and a Level-Set Method". In: **Journal of Computational Physics** 194.1, pp. 363–393.
- Bikas, H., P. Stavropoulos, and G. Chryssolouris (2016). "Additive Manufacturing Methods and Modelling Approaches: A Critical Review". In: **The International Journal of Advanced Manufacturing Technology** 83.1-4, pp. 389–405.
- DebRoy, T. et al. (Mar. 2018). "Additive Manufacturing of Metallic Components Process, Structure and Properties". In: **Progress in Materials Science** 92, pp. 112–224.
- Ding, Donghong et al. (2015). "A practical path planning methodology for wire and arc additive manufacturing of thinwalled structures". In: **Robotic and Computer-Integrated Manufacturing** 34, pp. 8–19.
- Henrot, Antoine and Michel Pierre (2018). **Shape Variation and Optimization**. Vol. 28. EMS Tracts in Mathematics. European Mathematical Society (EMS), Zürich.
- Liu, Jikai et al. (June 2018). "Current and Future Trends in Topology Optimization for Additive Manufacturing". In: **Structural and Multidisciplinary Optimization** 57.6, pp. 2457–2483.

Références II

Megahed, Mustafa et al. (Dec. 2016). "Metal Additive-Manufacturing Process and Residual Stress Modeling". In: **Integrating Materials and Manufacturing Innovation** 5.1, pp. 61–93.

Roberts, I. A. et al. (Oct. 2009). "A Three-Dimensional Finite Element Analysis of the Temperature Field during Laser Melting of Metal Powders in Additive Layer Manufacturing". In: **International Journal of Machine Tools and Manufacture** 49.12-13, pp. 916–923.

Van Belle, Laurent (2013). "Analyse, Modélisation et Simulation de l'Apparition de Contraintes En Fusion Laser Métallique". PhD thesis.

Wendl, S., H. J. Pesch, and A. Rund (2010). "On a State-Constrained PDE Optimal Control Problem Arising from ODE-PDE Optimal Control". In: ed. by Moritz Diehl et al., pp. 429–438.